



Oct 18th, 12:00 AM

Fatigue Behaviour of Cold-formed Steel Sections

Dimos Polyzois

Glenn Morris

S. K. Hassan

Follow this and additional works at: <https://scholarsmine.mst.edu/isccss>

 Part of the [Structural Engineering Commons](#)

Recommended Citation

Polyzois, Dimos; Morris, Glenn; and Hassan, S. K., "Fatigue Behaviour of Cold-formed Steel Sections" (1994). *International Specialty Conference on Cold-Formed Steel Structures*. 2.
<https://scholarsmine.mst.edu/isccss/12iccfss/12iccfss-session10/2>

This Article - Conference proceedings is brought to you for free and open access by Scholars' Mine. It has been accepted for inclusion in International Specialty Conference on Cold-Formed Steel Structures by an authorized administrator of Scholars' Mine. This work is protected by U. S. Copyright Law. Unauthorized use including reproduction for redistribution requires the permission of the copyright holder. For more information, please contact scholarsmine@mst.edu.

FATIGUE BEHAVIOUR OF COLD-FORMED STEEL SECTIONS

S.K. Hassan ^a, D. Polyzois ^b, and G. Morris ^c

SUMMARY

In the expected life span of a transmission tower, the members are subjected to a large number of alternating wind applications. Fatigue behaviour due to repeated loading must therefore be considered in design. This paper presents the fatigue-test results for 52 cold-formed steel members. The results obtained can be used to establish additional guidelines for fatigue design of cold-formed steel sections.

1. INTRODUCTION

Metal fatigue is a process which causes failure or damage of a component subjected to repeated loading. It is a complicated metallurgical process which is difficult to describe accurately and model precisely on a microscopic level. Despite these complexities, fatigue damage assessment for design of components and structures must be performed. If a structure is subjected to cyclic or repeated loading, it may fracture at a stress level less than that required to cause failure under static conditions. Fatigue failures are characterized by the progressive growth of cracks initiated from micro-flaws, in areas of tensile stress. This crack growth may continue to develop until the member cross section is so reduced in area that fracture occurs. The Canadian Standard¹ and the American LRFD-AISC Specification⁹ provide an extensive list of design conditions and situations into several stress range categories. No information is given regarding the fatigue design of cold-formed components.

Hydroelectric transmission towers are one example of structures which must not only be designed to withstand a wide range of loading conditions, but also be lightweight and maintenance free. The high strength-to-weight ratio, the simplicity of fabrication, and the ease of erection have made cold-formed steel an attractive material for the construction

^aPh.D. Candidate, Dept. of Civil and Geological Eng., Univ. of Manitoba, Winnipeg, MB., CANADA, R3T 5V6.

^bAssoc. Prof., Dept. of Civil and Geological Eng., Univ. of Manitoba, Winnipeg, MB., CANADA, R3T 5V6.

^cProf., Dept. of Civil and Geological Eng., Univ. of Manitoba, Winnipeg, MB., CANADA, R3T 5V6.

of such structures. During the expected service life of a transmission tower (50 years), it is subjected to hundreds of thousands of fluctuating wind applications. In addition, these towers are severely exposed to a large range of temperature change and other environmental and climatic conditions. As such, the need for studying the fatigue behaviour of cold-formed steel members is now becoming a growing concern.

Nowhere in the available literature has there been an extensive systematic investigation of the axial fatigue behaviour of cold-formed steel members. However, a large body of research in the area of fatigue of mechanical and aeronautical structures exists. It is only recently, that fatigue became important to the context of civil engineering practices. An experimental program⁷ conducted at the US Steel Corporation Research Laboratory, involved 24 beam specimens fabricated from sheet steel. This study indicated that the fatigue life of cold-formed sections was higher than that predicted by fatigue-design curves developed on the basis of tests on hot-rolled sections. The study also showed that fatigue life is a function of the fabrication details and that it may be decreased substantially if holes or welds are present. Research carried out by Libertini et al.⁸, has revealed that cold working of sheet-steel can improve the large cycle fatigue resistance, but may result in the degradation of small cycle fatigue resistance.

1.1 Wind Induced Fatigue Damage

Wind is considered a time-variant loading which may cause considerable number of significant stress fluctuations during the typical lifetime of a tower-type structure. Davenport², discussed the effect of a gusty wind on a simple elastic structure having one degree of freedom. He then expanded his investigation³ to include line-like structures (suspension bridges, tall masts, and overhead power lines) and developed general expressions for the response of such structures to gusty winds. In 1967, Davenport⁴ formulated factors which take proper recognition of the dynamic effect of wind on structures such as tall buildings, towers, and bridges.

An assessment of the sensitivity of lattice towers to fatigue induced by wind gusts was studied by Wyatt¹⁵. Other researchers in the field^{10, & 14} investigated the susceptibility of surface elements of high rise buildings to fatigue due to wind buffeting. Their procedure was based on the combination of meteorological data, fluctuating response of the surface elements, and S-N curves in conjunction with Palmgren-Miner's rule for cumulative damage.

1.2 Fatigue at Low Temperatures

Fatigue behaviour at low temperatures has received much less attention than that at room and elevated temperatures. Comprehensive summaries of S-N fatigue behaviour of

some metals at low temperatures were introduced by Teed¹³, and Forrest⁶. Their prime objective was to provide a general trend for long-life fatigue strengths at low temperatures (-40°C to -196°C) compared to room temperature. However, stress concentration factors were not correlated in the study. Spretnak et al.¹¹, performed low temperature fatigue tests on notched and unnotched specimens. The results showed that at short lives, low temperatures are usually beneficial to constant amplitude unnotched S-N fatigue behaviour, while at longer lives, notched fatigue strength are usually slightly better or similar to room temperature values. Studies concerning strain-life (ϵ -N) low cycle fatigue behaviour, indicated that long-life fatigue resistance is increased at low temperatures, while short-life fatigue resistance may decrease as a result of low ductility and low fracture toughness. Depending on the type of steel material, low temperatures can be beneficial or detrimental or have a little influence on the total fatigue life of a component.

2. EXPERIMENTAL INVESTIGATION

The primary objective of the experimental program was to investigate the axial fatigue behaviour of full-size cold-formed steel members typical of those used for constructing transmission towers. Assurance was made to simulate loading and environmental conditions similar to those encountered in service. The experimental program involved the use of five cross sectional shapes and two test temperatures, -50°C and 25°C . A total of 52 constant amplitude fatigue tests were performed under load-controlled conditions with a load ratio of -1 (fully reversed load cycle). Of these, 42 specimens were fabricated from A715 Grade 60 steel by SAE in Milan, Italy, and the remaining 10 specimens were fabricated from G40.21-300W steel ($F_y \simeq 44 \text{ ksi}$) in Canada. The total length of all test specimens was 1500 mm. Actual dimensions of each specimen were recorded on an observation sheet prior to testing. A three-character designation system was used to identify test specimens and their category. The first character identifies the specimen's shape (BA, BB, BC, BG, and BN). The second character is the nominal slenderness ratio ($\frac{L}{r_{cr}}$) of the section. The third character is the number of the test specimen within its category. G40.21 steel specimens were identified by the letter "H" preceding the shape identifier. The names and dimensions of the different cross sections are illustrated in Figure 1.

Prior to fatigue testing, static tension tests were first performed on three cross sections (BA, BB, and BC) to determine their ultimate tensile capacities at room temperature. Ratios of the obtained capacity were then used in the fatigue testing of the specimens. A detailed summary of the number of fatigue tests performed for each cross section, the test temperatures, and the steel material types involved in the study is given in Table 1.

The specimens were tested in a temperature-controlled chamber where a temperature of -50°C could easily be achieved and maintained. All specimens were connected to a $\frac{1}{2}$ in. (13 mm) thick gusset plate, through the use of properly tightened A490 structural bolts $\frac{5}{8}$ in. (16 mm) diameter, to assure slip-resistant (friction type) connections during

cyclic loading. The loading was controlled by an MTS-5000 kN capacity closed loop testing machine. A second MTS-1000 kN capacity was also employed to test ten back-to-back channel specimens at room temperature. The number of cycles of loading and unloading was recorded by a cycle counter. Photographs of the test set-ups are shown in Figure 2.

The instrumentation mainly consisted of four Linear Variable Differential Transducers (LVDT's) located at the midheight section of the specimens to record the lateral and rotational displacements. In addition, electrical resistance strain gauges were mounted on the test specimen at the top and bottom connections to monitor the cyclic stress-strain behaviour. An amplifier was used in conjunction with the strain gauges to eliminate any noise in the signal. Moreover, a thermocouple was connected to the specimen to monitor the temperature in the cooling-chamber. All data was recorded through the use of an automatic data acquisition system.

3. EXPERIMENTAL RESULTS

True stress control can easily be achieved only at small deformations. Stress control, however, becomes unmanageable when cracks form in the material. Thus, load was chosen as the control function. A triangular wave form was adopted in this study with a load ratio of -1 as shown in Figure 3 (fully reversed load cycle). The obtained stress ratio (R) for all sections ranged from 0.87 to 0.93. Test frequency ranged from 1 Hz. to 2.5 Hz. depending on the stroke level. The stress range σ_r is considered the most important non-geometric variable in studies concerning the total fatigue life.

3.1 Crack Initiation and Growth

For all tested specimens, the crack initiation and growth patterns were similar. Initial cracking began at the extremity of one of the end holes and proceeded to grow under cyclic loading until fracture occurred at the net section at either the top or bottom connection. The degree and extent of damage observed varied among the specimens tested. The exceptions were three block-shear failures for the 90°-angle specimens (BA-109-4, 9, and 8) connected through one leg. Those failures were observed at high stress range levels (95, 102, and 118 ksi or 653, 707, and 813 MPa) respectively. Another exception was for the 60°-angle section which witnessed gross section failures located at 60 mm from the mid-height section. Such failures were mainly due to the presence of high stress concentrations caused by an engraved letter at the back of the angles.

For the back-to-back channel section (BN-36-3) tested at room temperature, failure occurred at both sides of the member. A fatigue crack first originated at the extremity of the end hole at the top right member and continued to grow towards the flanges followed by a sudden fracture of the left member at the location of the lower spacer plate which

was used to tie the two channels together. Another example of compound fatigue failure was observed for HBN-37-9 tested at a temperature of -50°C where two cracks originated at both the top and bottom connections on one side of the member.

3.2 Cyclic Stress-Strain Behaviour

Cycle-dependent softening was observed for all tested specimens, this was evidenced by the exponential increase of strains as the number of cycles increased. The runaway nature of the process is clearly shown in the cyclic stress-strain loops given in Figures 4 to 10. Stiffness reduction was observed for all specimens at final stages of the fatigue life as a result of the formation of large irrecoverable plastic strains. These strains can be related to fatigue damage much better than can other factors present in the fatigue problem. The area inside a loop represents the work done or the energy dissipated for a given stress range.

The effect of low temperature (-50°C) on the cyclic behaviour of the back-to-back channel section is shown in Figure 10. For the five tested specimens a noticeable decrease in the stroke took place from the beginning of the test until almost half the fatigue life was reached. That reduction ranged from 0.8% to 2% of the initial stroke of the specimen recorded at the first few cycles. The stroke then increased by increasing the number of cycles until failure occurred. For specimens HBN-37-8, 9, and 10, very short crack sizes were observed at fracture. This was mainly attributed to large reductions in fracture toughness and ductility that take place at low temperatures. Crack initiation process covered almost the entire low temperature fatigue life. Moreover, crack propagation rates were so high and occurred at a short period of time causing the sudden brittle fracture of the specimen.

3.3 S-N Curves

The plot between the stress range σ_r versus the total fatigue life is commonly referred to as S-N curves. Life steadily increases with decreasing stress until the fatigue limit is reached. It may suffice to say that in this study the concept of fatigue strength was used. The fatigue limit was defined as the stress range corresponding to a minimum of 10^6 cycles. The number was based on an expected life of 50 years for a transmission tower and a maximum of 50 alternating wind applications per day which gives a total of approximately 920,000 cycles.

In dealing with S-N curves, at least a brief mention must be made of scatter in individual data points which mainly increases with increasing life range. The reason of this scatter is associated with the exponential nature of the fatigue problem. A study conducted at the University of Surrey, England by Sweeting¹², presented a method of constructing safe S-N curves. This method has been incorporated into recent guidelines for compliance with design and airworthiness requirements.

For the purpose of comparing the results obtained from the S-N curves, a regression analysis was performed for the different test series. The governing log-log relationship is given in the form:

$$\log N = A - B \log \sigma_r \quad (1)$$

$$\text{or } N = \frac{10^A}{\sigma_r^B} \quad (2)$$

where, σ_r is the stress range in MPa, A and B are constants used to provide a best fit line to the fatigue data. B is the slope of the log-log S-N curve which ranges between 3 and 4.5 for most structural details. A similar relationship was obtained for the alternating fatigue load versus the number of cycles to failure.

S-N curves for singly symmetric sections connected through one leg (BA, BC, and BB sections) at room temperature of 25°C are shown in Figure 11. For a given number of cycles, the fatigue strength of the BA section was 4.5% higher than that of the BC section and 30% higher than that of the BB section. The performance of the 60°-angle sections connected through both legs is shown in Figure 12. These specimens showed an increase in the fatigue strength of about 12% compared to corresponding specimens connected only through one leg. S-N curve for the BG-section was 5% lower than that of the 90°-angle section connected through one leg as shown in Figure 13. Other S-N plots of BN and HBN-sections at 25°C, and HBN-sections at temperature of -50°C, are shown in Figure 14. The difference in steel types between BN and HBN sections resulted in an obvious change in the slope of the curves. At a given number of cycles, fatigue tests performed for HBN sections at -50°C, showed 11.5% increase in the stress range compared to room temperature tests as illustrated in Figure 14.

CONCLUSIONS

The following conclusions are based on the evaluation of experimental test data from 52 full-size cold-formed steel members tested under constant amplitude axial fatigue loads.

1. The fatigue behaviour defined in this study was between 10^4 and 10^6 cycles. The endurance limit (fatigue limit) was defined as the stress range level corresponding to a minimum of 10^6 cycles.
2. Fatigue loads were applied in a triangular wave form in a fully reversed load cycle. The shape of the wave form is not a critical variable and attention is rather focused on the upper and lower peaks of loading. The testing frequency ranged from 1 Hz. to 2.5 Hz. depending on the stroke level of the specimen.

3. The stress range was the dominant stress variable influencing the fatigue behaviour of cold-formed steel sections tested during this study. Other stress variables, such as minimum stress, maximum stress, and the stress ratio did not appear to have a significant effect on the sections.
4. Most failures occurred at the extremity of the end hole of the tested specimens as shown in Figure 15.
5. Cycle-dependent softening was observed for all tested specimens, that was evidenced by the exponential increase of strains as the number of cycles increased.
6. In comparing the fatigue performance of the sections, it was observed that the 90°-angle section can withstand 4.5% higher stress range than the 60°-angle section and 30% higher than the lipped-angle section.
7. Considering alternating fatigue loads, the BB-section sustained 36% higher load than the BC-section and 60% higher than the BA-section.
8. Better fatigue performance was observed for singly symmetric sections connected through both legs compared to similar specimens connected only through one leg. For a given number of cycles, the average increase of stress range was 25% for the 90°-angle section, 15% for the 60°-angle section, and 12% for the lipped-angle section.
9. The fatigue limit for the T-shaped section was obtained by extrapolating the log-log relationships to the level of $N = 10^6$ cycles. Stress range and the corresponding alternating fatigue load at that limit were 40 ksi (276 MPa) and ± 29.5 Kips (± 131 kN).
10. Fatigue tests performed at a temperature of -50°C indicated that the crack initiation process covered almost the entire low temperature fatigue life. Fractures associated with very short crack sizes were attributed to large reductions in fracture toughness and ductility associated with low temperatures.
11. Fatigue tests performed on HBN sections at a temperature of -50°C showed 11.5% increase in the stress range level compared to similar specimens tested at room temperature.
12. For each test series, a log-log linear relationship between the stress range and the number of cycles was developed. The log-transformation of the curves resulted in a normal distribution of the test data at all levels of stress range.
13. The mean regression line for S-N curves of steel type ASTM A715 Grade 60 had an average negative slope of approximately 4.5. The corresponding value for steel type CSA-G40.21-300W was 3.65. Slope values obtained by Fisher et al.⁵ in evaluating the fatigue strength of steel beams with welded stiffeners and attachments ranged between 3.1 and 3.5 for ASTM A514 steel material.

ACKNOWLEDGMENT

This experimental program was conducted at The Structural Engineering and Construction Research and Development Facility of The Civil and Geological Engineering Department, The University of Manitoba. The financial assistance provided by the Canadian Electric Association (CEA - Project No. 340 T 844 : *Use of Cold-Formed Steel Sections for Transmission Towers in Canada*), and Manitoba Hydro is greatly appreciated.

Appendix I. REFERENCES

1. CSA CAN3-S16.1-M89, (1989). *"Steel Structures for Building - Limits States Design"*, Canadian Standards Association, Rexdale, Ontario.
2. Davenport, A.G., (1961). *"The Application of Statistical Concepts to the Wind Loading of Structures"*, Proceedings, Institution of Civil Engineers, London, Vol. 19, p.449.
3. Davenport, A.G., (1962). *"The Response of Slender Line-Like Structures to a Gusty Wind"*, Proceedings, Institution of Civil Engineers, London, Vol. 23, p.389.
4. Davenport, A.G., (1967). *"Gust Loading Factors"*, J. Struct. Div., ASCE, Vol. 93, No. ST3.
5. Fisher, J.W., Albrecht, P.A., Yen, B.T., Klingerman, D.J., and McNamee, B.M. (1974). *"Fatigue Strength of Steel Beams with Welded Stiffeners and Attachments"*, NCHRP Report 147, Washington, D.C., 85 pp.
6. Forrest, P.G., (1963). *"Fatigue of Metals"*, Pergamon Press, Elmsford, New York.
7. Klippstein, K.H., (1981). *"Fatigue Behaviour of Sheet Steel Fabrication Details"*, Soc. Automotive Engineers, Paper No. 810436.
8. Libertini, G.Z., Topper, T.H., and Leis, B.N., (1977). *"The Effect of Large Prestrain on Fatigue"*, Experimental Mechanics.
9. Manual of Steel Construction, (1986). *"Load and Resistance Factor Design"*, American Institute of Steel Construction, (AISC), Chicago, Illinois.
10. Patel, K., and Freathy, P., (1984). *"A simplified Method for Assessing Wind-Induced Fatigue Damage"*, Eng. Struct., Vol. 6, p.268.
11. Spretnak, J.W., Fontana, M.G., and Brooks, H.E., (1951). *"Notched and Unnotched Tensile and Fatigue Properties of Ten Alloys at 25°C and -196°C"*, Trans., ASME, Vol. 43, p. 547.
12. Sweeting, T.J., (1992). *"A Method for the Construction of Safe S-N curves"*, Fatigue Fract. Engng Mater. Struct., Vol. 15, No. 4, pp. 391-398.






13. Teed, P.L., (1950). *"The Properties of Metallic Materials at Low Temperatures"*, Chapman and Hall.
14. Wacker, J., and Plate, E.J., (1990). *"Fatigue Caused by Wind Buffeting on Surface Elements of High Rise Buildings"*, Structural Dynamics, Rotterdam, p.1133.
15. Wyatt, T.A., (1984). *"An Assessment of the Sensitivity of Lattice Towers to Fatigue Induced by Wind Gusts"*, Eng. Struct., Vol. 6, p.262.

Appendix II. NOTATION

The following symbols were used in this paper :

- A = constant to provide a best fit line to the fatigue data;
 B = the negative slope of the log-log curve;
 L = total length of all fatigue test specimens (1500 mm);
 N = number of cycles;
 R = stress ratio, (ratio of the minimum stress to the maximum stress);
 r_{cr} = minimum radius of gyration of a cross section;
 σ_r = stress range in Mpa, (algebraic difference of the maximum and minimum stresses applied to a test specimen).

Table 1 : Number of Specimens and Test Variables

Section	BA		BC		BB		BG		BN**	
										
Test Variables	Th. = 4 mm		Th. = 4 mm		Th. = 4 mm		Th. = 4 mm		Th. = 5 mm	
	No. of Sp.	Length (mm)	No. of Sp.	Length (mm)	No. of Sp.	Length (mm)	No. of Sp.	Length (mm)	No. of Sp.	Length (mm)
(ASTM) A 715 Grade 60	ROOM TEMP.		13*	1500	13*	1500	8*	1500	3	1500
	TEMP. -50 C								5	1500
			TOTAL = 42							
(CSA) G 40.21 Grade 300W	ROOM TEMP.								HBN	5 1500
	TEMP. -50 C								HBN	5 1500
			TOTAL = 10							
Nominal Slenderness Ratio (L/r)	109		81		70		36		36 - 37	

* Three specimens were tested with both legs connected.

** No. of specimens for "BN" and "HBN" sections refers to a section composed of 2 channels.

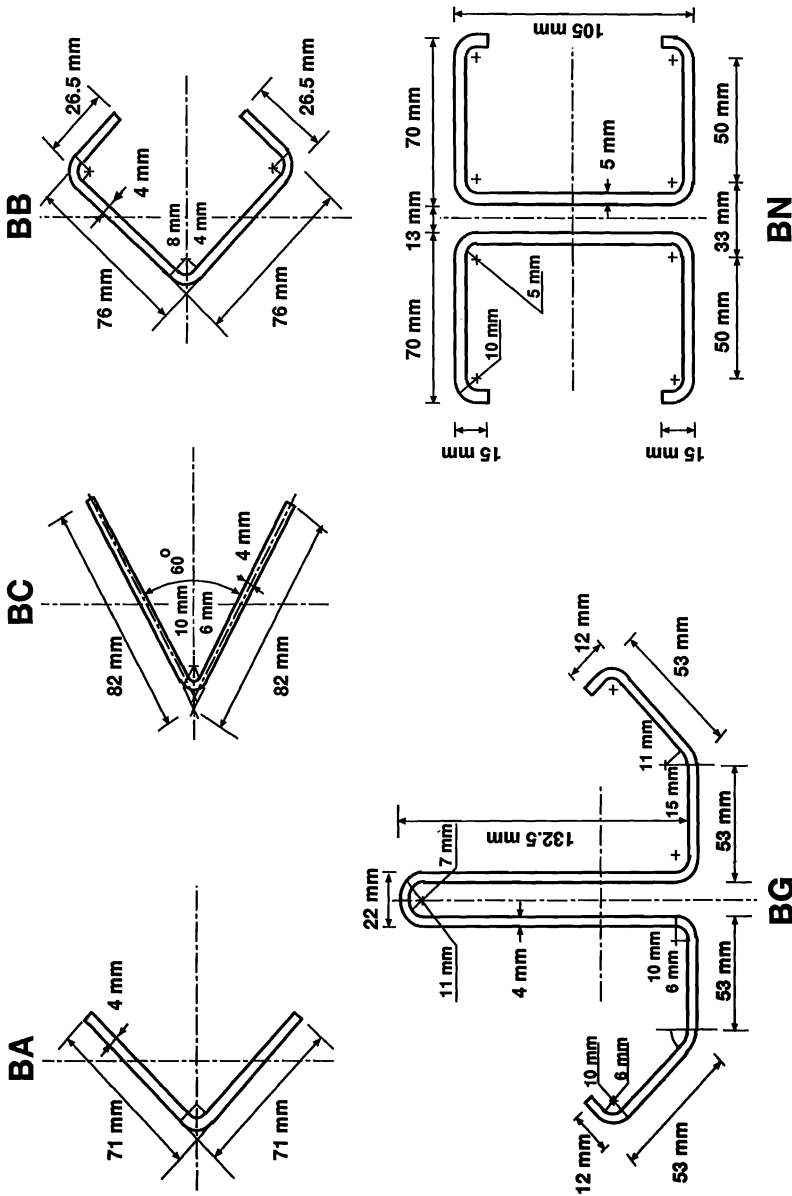
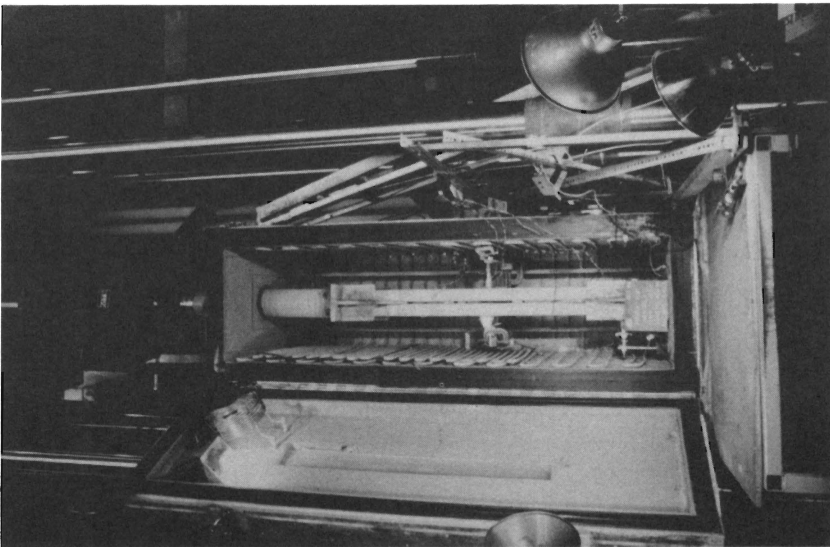
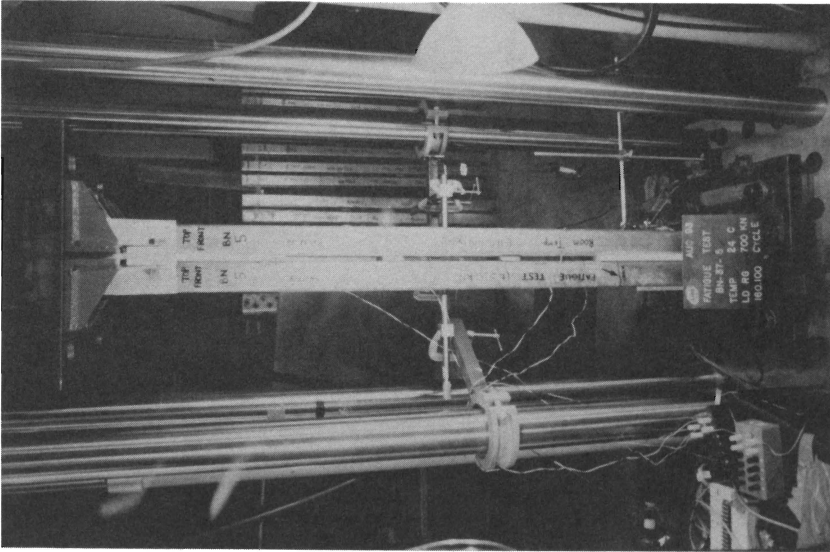


Figure 1 : Nominal Cross Sectional Dimensions



a) MTS - 5000 kN Testing Machine



b) MTS - 1000 kN Testing Machine

Figure 2 : Fatigue Test Set-ups

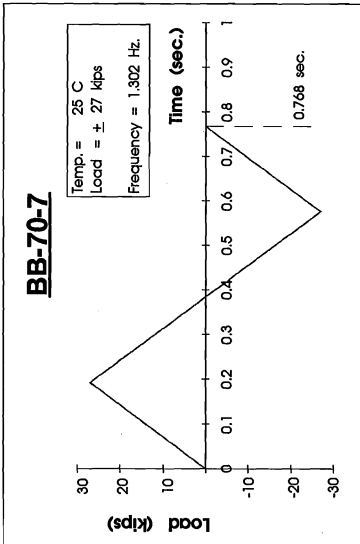
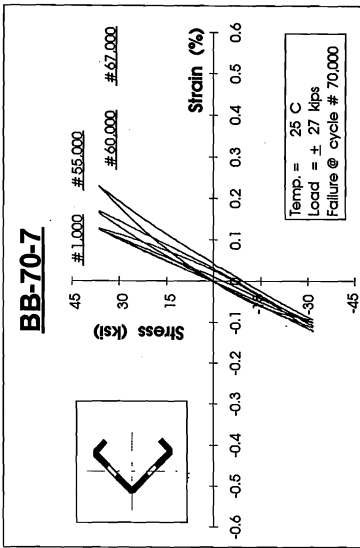
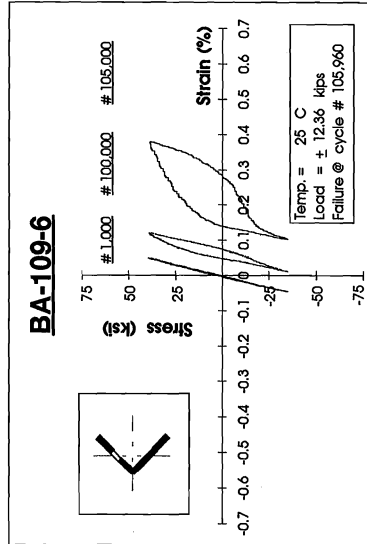
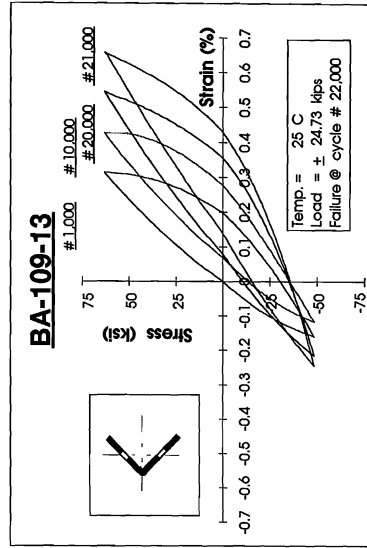


Figure 3 : Cyclic Loading Frequency

Figure 4 : Stress-Strain Loops for the Lipped angle Section
(Both Legs Connected)Figure 5 : Stress-Strain Loops for the 90° angle Section
(One Leg Connected)Figure 6 : Stress-Strain Loops for the 90° angle Section
(Both Legs Connected)

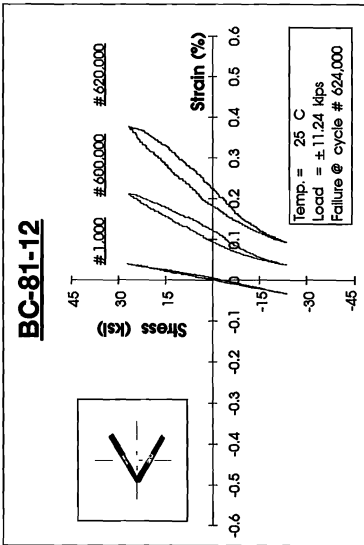


Figure 7 : Stress-Strain Loops for the 60°-angle Section
(Both Legs Connected)

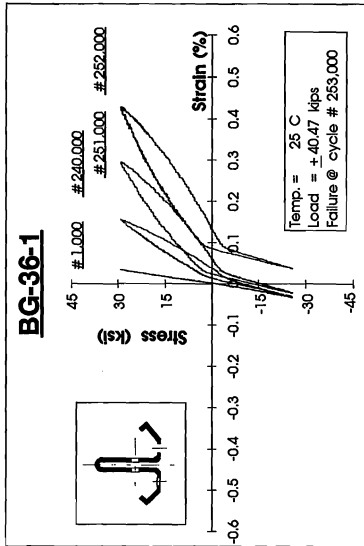


Figure 8 : Stress-Strain Loops for the T - shaped Section

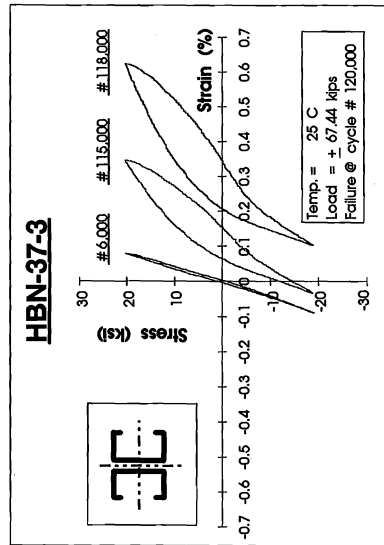


Figure 9 : Stress-Strain Loops for the Back-to-Back
Channel Section Tested at 25°C

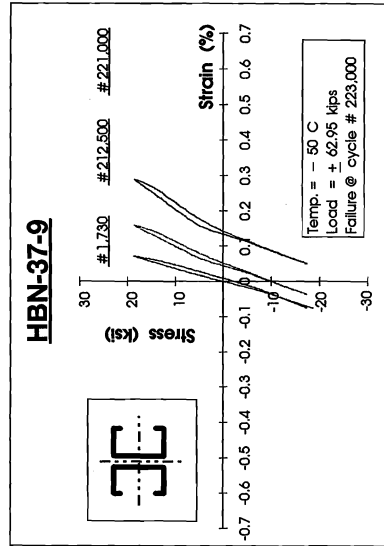
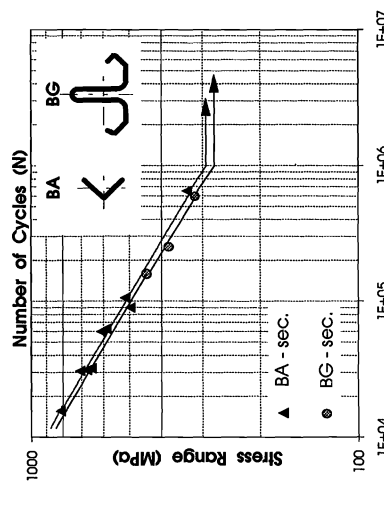
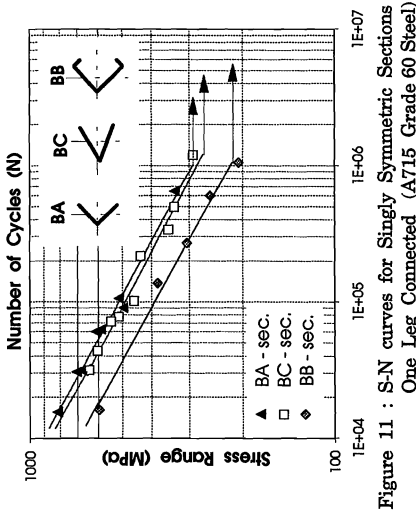
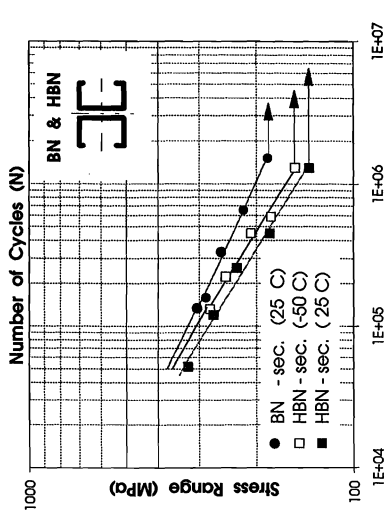
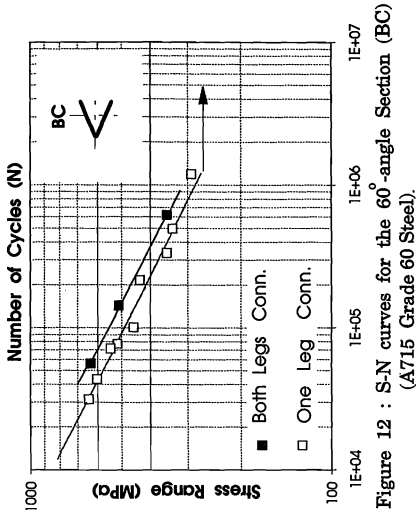


Figure 10 : Stress-Strain Loops for the Back-to-Back
Channel Section Tested at -50°C



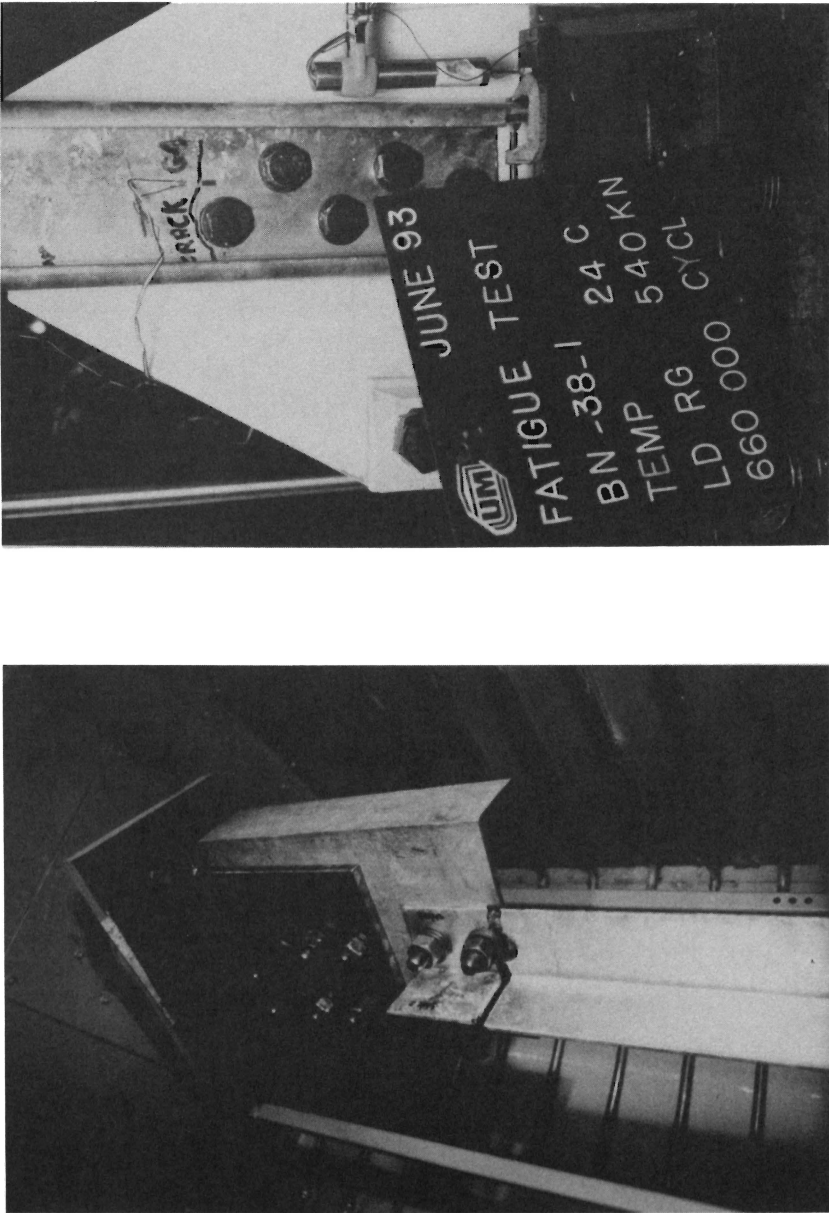


Figure 15 : Fatigue Test Specimens at Failure

